

## SPECTROSCOPIC AND THERMAL STUDY OF BENTONITES FROM MILOS ISLAND, GREECE

Bourliva A.<sup>1</sup>, Michailidis K.<sup>1</sup>, Sikalidis C.<sup>2</sup> and Filippidis A.<sup>1</sup>

<sup>1</sup> Department of Mineralogy-Petrology-Economic Geology, School of Geology, Aristotle University of Thessaloniki, 54124 Thessaloniki, Greece, [annab@geo.auth.gr](mailto:annab@geo.auth.gr)

<sup>2</sup> Department of Chemical Engineering, Aristotle University of Thessaloniki, 54124 Thessaloniki Greece

### Abstract

*Bentonitic clays, currently in use in over hundred areas, are among the most important industrial raw materials. In most of the cases, bentonites predominantly consist of montmorillonite which is a 2:1 layer clay mineral formed by one alumina octahedral sheet placed between two silica tetrahedral sheets. Three bentonite composite samples (BN1, BN2, BN3) with some differences in mineralogical and chemical composition from Milos island ("Miloan"), Greece were investigated by X-ray diffraction (XRD), atomic absorption spectrometry (AAS), differential thermal analysis (DTA), thermogravimetric analysis (TG), Fourier transform infrared (FTIR) and surface area (BET) measurements techniques. Mineralogically, bentonite samples were characterized by high concentrations of smectite (>85%) and minor amounts of other clay minerals (illite and kaolinite). Nonclay minerals such as quartz, calcite and pyrite were also identified. The infrared spectrum of the bentonites also revealed the presence of dioctahedral smectite as the major component and quartz as the main impurity in all the samples. The stretching vibration at  $3698\text{cm}^{-1}$  in the sample BN3 could be ascribed to kaolinite. DTA-TG curves of all samples were measured in the temperature range 75-1000°C. The total weight losses for the bentonite samples BN1, BN2 and BN3 were determined as 16.25, 12.32 and 13.35% respectively.*

**Key words:** smectite, Milos, FTIR, DTA/TG.

### Περίληψη

Ο μπεντονίτης, με πληθώρα εφαρμογών και χρήσεων, αποτελεί μια από τις σημαντικότερες βιομηχανικές πρώτες ύλες. Στις περισσότερες περιπτώσεις, ο μπεντονίτης αποτελείται κυρίως από μοντμοριλλονίτη, ένα 2:1 αργιλικό ορυκτό με δομή που αποτελείται από ένα οκτάεδρο αργιλίου που τοποθετείται μεταξύ δύο τετραέδρων πυριτίου. Τρία σύνθετα δείγματα μπεντονίτη (BN1, BN2, BN3) με διαφορές τόσο στην ορυκτολογική όσο και στην χημική σύσταση από το νησί της Μήλου, μελετήθηκαν με την μέθοδο της περιθλασιμετρίας ακτίνων-X (XRD), με την μέθοδο της φασματοσκοπίας ατομικής απορρόφησης (A.A.S.), με διαφορική θερμική (DTA) και θερμοσταθμική ανάλυση (TG), με φασματοσκοπία υπέρυθρης ακτινοβολίας με μετασχηματισμούς Fourier (FTIR) και με μετρήσεις της ειδικής επιφάνειας (BET). Ορυκτολογικά τα δείγματα χαρακτηρίζονται από υψηλό ποσοστό σμεκτίτη (>85%) και μικρά ποσοστά άλλων αργιλικών ορυκτών (ιλλίτης και καολίνιτης). Προσδιορίστηκαν,

*επίσης, χαμηλά ποσοστά μη αργιλικών ορυκτών όπως χαλαζία, ασβεστίτης και σιδηροπυρίτης. Το υπέρυθρο φάσμα των δειγμάτων επιβεβαίωσε την παρουσία του διοκταεδρικού σμεκτίτη ως κύριου συστατικού και του χαλαζία ως κύριας πρόσμιξης σε όλα τα δείγματα. Η δόνηση στα  $3698\text{cm}^{-1}$  στο δείγμα BN3 αποδόθηκε στην παρουσία καολινίτη. Οι καμπύλες DTA/TG όλων των δειγμάτων μετρήθηκαν στο θερμοκρασιακό εύρος  $75-1000^\circ\text{C}$ . Οι συνολικές απώλειες βάρους προσδιορίστηκαν σε 16.25, 12.32 και 13.35% για τα δείγματα BN1, BN2 και BN3, αντίστοιχα. Λέξεις κλειδιά: μοντοριλλονίτης, Μήλος, FTIR, DTA/TG.*

## 1. Introduction

Bentonite, currently in use in over a hundred areas, is among the most important industrial raw materials (Grim and Goven, 1978; Murray, 2000). The dominant mineral in bentonite is montmorillonite which belongs to the smectite group (Grim and Goven, 1978). Smectite is a 2:1 layer clay mineral and has two silica tetrahedral sheets bonded to a central alumina octahedral sheet. Smectites are described either as dioctahedral or as trioctahedral depending upon whether the octahedral cations are predominantly trivalent or divalent, respectively. The net negative electric charge of the 2:1 layers arising from the natural isomorphic substitution of  $\text{Fe}^{2+}$  and  $\text{Mg}^{2+}$  for  $\text{Al}^{3+}$  in the octahedral sites and  $\text{Al}^{3+}$  for  $\text{Si}^{4+}$  in tetrahedral sites is balanced by the presence of exchangeable cations such as  $\text{Na}^+$  and  $\text{Ca}^{2+}$  located between the layers and surrounding the edges (Murray, 2000).

Bentonites are among the most important industrial raw materials and have wide range of uses in many industrial applications like oil, petroleum, cosmetics, ceramics and paintings (Murray, 1991). The application areas of bentonites depend on the quality and quantity of their smectites and other clay and non-clay mineral constituents (Grim, 1968). Some physico-chemical properties of bentonites as well as their mineralogy are greatly affected by thermal treatment. Due to these effects, the investigation of thermal behavior of bentonite samples is of great importance. Additionally, spectroscopic (FTIR) investigation in clay mineral speciation was recently regarded as a useful tool with a multipurpose application, since some physical details of clay lattices and experimental qualitative correlation between the samples were made possible (Davarcioğlu and Çiftçi, 2009).

Greek bentonite is mainly quarried in the north-eastern part of the island, where some of the economically most important bentonite deposits in Europe are concentrated (Kogel et al., 2006). The deposits have been formed by the alteration of Lower Pleistocene volcanoclastic rocks (Christidis et al., 1995). The bentonite reserves are estimated to exceed 20Mt and along with United States, Greece is one of the largest exporters of bentonites. Previous studies on the Miloan bentonites performed at different stages of quarry development, referred on their mineralogy, mode of formation and on their physical properties (Christidis et al., 1995; Christidis and Markopoulos, 1995; Christidis and Scott, 1996; Perraki and Orphanoudaki, 1997). Since information on the evolution of the smectite characteristics in space is very important, representative samples of the Miloan bentonites were used in this investigation. Thus, the aim of this study was to present new data concerning the mineralogical, structural and thermal properties of bentonites from Milos island.

## 2. Materials and Methods

### 2.1. Bentonite Samples

Three natural bentonite samples from W.Ankeria, N.Aspro Horio and S.Aspro Horio deposits of Milos island, coded as BN1, BN2 and BN3 respectively, were used in the present study. The samples were provided by the S&B Industrial Minerals S.A. The samples, were ground, sieved to

obtain the <63 $\mu\text{m}$  particle size fraction, washed with distilled water to remove the soluble salts possibly present and air dried before the experiments.

## 2.2. Analytical Methods and Instrumentation

Chemical analyses of the rock samples were performed by AAS using a Perkin Elmer 5000 apparatus. Sample was crushed in an agate mill till a size <20  $\mu\text{m}$ . Then dried for a whole night at 105°C. 200 mg of powdered bentonite, weighed with a precision of  $\pm 0.03$  was placed in Teflon autoclaves. Sample dissolution was achieved with the addition of 10 mL HF, 2 mL H<sub>2</sub>SO<sub>4</sub> and 1 mL HClO<sub>3</sub>. The autoclaves were heated at 110°C for 60 min. After being cooled in tap water for about 30 min, 5 g of H<sub>3</sub>BO<sub>3</sub> were quickly added along with 30 mL of warm distilled water. The solution was stirred for 5–15 min on a magnetic plate. After this stage the solution was absolutely clear owing to complete dissolution. It was then transferred to a 250 mL volumetric flask, adjusted to volume and stored in a polyethylene container. From this solution Si, Al and Mn were determined with flame atomic absorption spectroscopy. 10 mL from the first solution was condensed in an open Teflon vessel until it was completely dry. Then 4 mL HCl 1:9 were added and left to evaporate (this procedure is done twice). Finally, after all the liquid has evaporated, 10 mL HCl 1:9 are added to the solid residue along with 1 mL dense HCl. The solution was transferred to a 100 mL volumetric flask along with 10 mL of 50 mg mL<sup>-1</sup> LaCl<sub>3</sub> solution. The solution was adjusted to 100 mL volume and was used to determine K, Na, Ca, Mg and Fe with flame atomic absorption spectroscopy. P and Ti were determined with a Spekol, Carl Zeiss simple beam spectrophotometer. Loss of ignition (LOI) was determined by heating 0.5–1 g of rock powder for 2 h at 1050°C. Detection limits in solution were: Si 1.8  $\mu\text{g mL}^{-1}$ , Al 1.0  $\mu\text{g mL}^{-1}$ , Fe 0.12  $\mu\text{g mL}^{-1}$ , Mn 0.055  $\mu\text{g mL}^{-1}$ , Mg 0.007  $\mu\text{g mL}^{-1}$ , Ca 0.08  $\mu\text{g mL}^{-1}$ , Na 0.015  $\mu\text{g mL}^{-1}$ , K 0.04  $\mu\text{g mL}^{-1}$ .

Mineralogical characterization of the bentonites as well as semi-quantitative mineral determination was performed by X-Ray powder diffraction (XRPD) using a Philips PW1710 diffractometer. Ni-filtered copper K $\alpha$  radiation was used energized to 35kV and 25mA, in the range 3–63°2 $\theta$  at a scan speed of 1.2°/min. The characterization of the mineral phases was performed semi-quantitatively on the basis of the intensity (counts) of specific reflections, density, and mass absorption coefficient (CuK $\alpha$ ) of the identified mineral phases.

Infrared spectra of the bentonite samples were recorded (4000–400cm<sup>-1</sup>) with Perkin-Elmer FTIR Spectrum 1000 spectrometer at a resolution of 4cm<sup>-1</sup> using KBr pellet technique. BET surface areas were calculated from the first part of the N<sub>2</sub> adsorption isotherm (P/Po<0.5) obtained at liquid nitrogen temperature with N<sub>2</sub> in Autosorb (Quantachrome Corporation) equipment. High-purity (99.99%) nitrogen was used in adsorption measurements. Simultaneous DTA/TG experiments were carried out using a TA Instrument SD 2960 thermal analyzer. Approximately 15 $\pm$ 2 mg of sample was used in each run. The samples were placed in an alumina crucible and an empty alumina crucible was used as a reference standard. All experiments were performed at a linear heating rate of 10°C min<sup>-1</sup> over the temperature range of 75–1000°C.

## 3. Results and Discussion

### 3.1. Chemical Analysis

The results of chemical analyses of bentonite samples are presented in Table 1. SiO<sub>2</sub> and Al<sub>2</sub>O<sub>3</sub> constitute the main oxides in the bentonites composition with contents ranging 52.92–60.24% and 16.97–18.33% respectively, whereas TiO<sub>2</sub>, MnO, K<sub>2</sub>O and P<sub>2</sub>O<sub>5</sub> are present only in small quantities. As shown in Table 1, the weight percent of calcium contained in the bentonite samples (1.39–3.05%) is higher than that of sodium (0.70–1.13%). The MgO content ranges between 1.78 and 4.30%. In both cases, the Fe<sub>2</sub>O<sub>3</sub> content is high (about 5–10%).

**Table 1 – Chemical analyses (wt %) of the bentonite samples.**

Chemical analysis	BN1	BN2	BN3
SiO <sub>2</sub>	56.83	60.24	52.92
Al <sub>2</sub> O <sub>3</sub>	16.97	18.33	18.04
TiO <sub>2</sub>	0.67	0.72	0.63
MnO	0.07	0.01	0.01
Fe <sub>2</sub> O <sub>3</sub>	5.72	5.17	10.62
MgO	4.30	3.30	1.78
CaO	3.05	2.02	1.39
Na <sub>2</sub> O	1.13	0.92	0.70
K <sub>2</sub> O	0.57	0.68	1.13
P <sub>2</sub> O <sub>5</sub>	0.08	0.04	0.13
L.O.I. (Loss Of Ignition)	10.63	8.60	12.40
<b>Total</b>	<b>100.02</b>	<b>100.03</b>	<b>99.75</b>

### 3.2. Mineralogical Analysis

The X-ray diffraction patterns of the bentonite samples are illustrated in Figure 1.

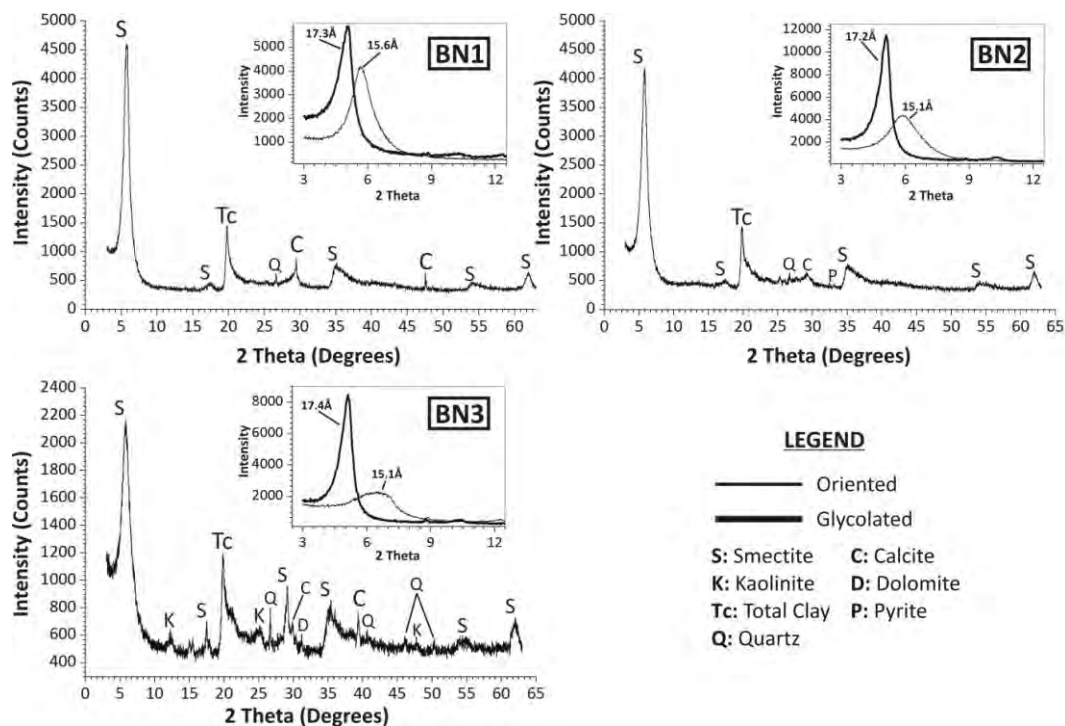


**Figure 1 – X-ray diffraction patterns of the bentonite samples (bulk samples). In the detail there are the patterns of the oriented and glycolated samples.**

Bentonites are mainly composed of dioctahedral smectite and specifically Ca-montmorillonite with the  $d_{001}$  basal reflection exhibited at about  $15\text{\AA}$  (Figure 1). The estimated smectite contents of the samples were found 94%, 97% and 88% for the samples BN1, BN2 and BN3, respectively. The BN3 sample additionally contains kaolinite ( $d_{001}=7.12\text{\AA}$ ,  $d_{002}=3.57\text{\AA}$ ). Accessory minerals such as quartz ( $d_{101}=3.34\text{\AA}$ ,  $d_{100}=4.26\text{\AA}$ ) and calcite ( $d_{104}=3.03\text{\AA}$ ) were detected in all samples. Minor amounts of pyrite ( $d_{200}=2.71\text{\AA}$ ) were present in BN2 bentonite, and traces of dolomite ( $d_{104}=2.88\text{\AA}$ ) in BN3 bentonite. Thus, bentonite samples are characterized by high concentration of smectite and low levels of impurities. Similar observations were reported by other authors (Christidis et al., 1995; Perraki and Orphanoudaki, 1997). According to Christidis et al. (1995) dioctahedral smectite is the main phase present in Ankeria and Aspro Horio deposits, while plagioclase is abundant, kaolinite, calcite and zeolites are secondary phases and sulphides are accessory minerals. Perraki and Orphanoudaki (1997) reported that Ankeria bentonite consists mainly of Ca-montmorillonite with minor amounts of calcite, feldspars, quartz, illite and iron sulphides (e.g. pyrite).

### 3.3. Specific Surface Area

The specific surface areas of bentonite samples were determined from the nitrogen adsorption isotherms given in Figure 2. The BET surface areas (obtained by  $N_2$  adsorption isotherms at 77 K) were 87, 67 and  $80\text{ m}^2/\text{g}$  for BN1, BN2 and BN3, respectively. BET surface areas of these samples were similar to those found for natural bentonites reported in previous workers (Volzone and Ortiga, 2000; Sakizci et al., 2010).

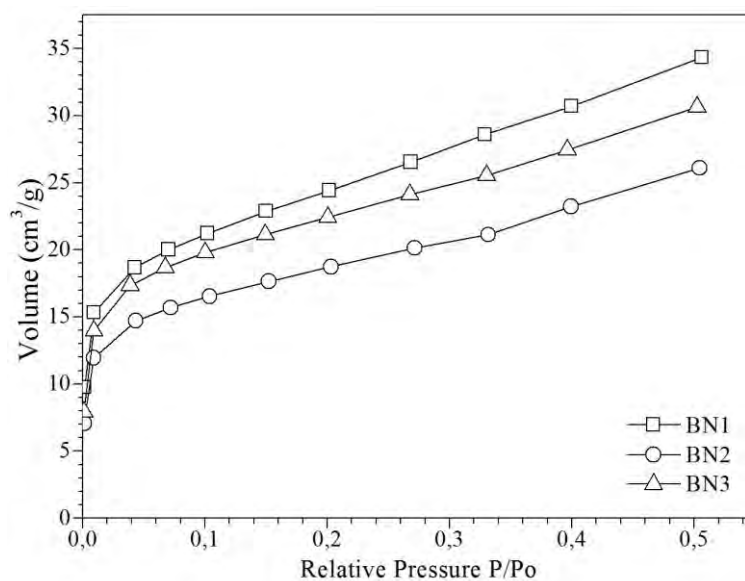


Figure 2 – The isotherms of the adsorption of nitrogen ( $N_2$ ) on the bentonite samples.

### 3.4. Spectroscopic Study

FTIR spectra of bentonite samples are shown in Figure 3 and the vibrational modes are summarized in Table 2 together with FTIR data of the Miloan bentonites from previous studies (Christidis et al., 1995; Orphanoudaki and Perraki, 1997) and Wyoming (Tabak et al., 2007) and Ünye, Turkey (Sakizci et al., 2010) bentonites for comparison. Position and shape of the OH stretching band in the IR spectra of smectites is influenced mainly by the nature of the octahedral atoms to which the hydroxyl groups are coordinated (Madejova, 2003).

The absorption band at  $3628$ ,  $3630$  and  $3622\text{ cm}^{-1}$  found in the spectra of BN1, BN2 and BN3 sample respectively, are typical for dioctahedral smectites and is due to stretching vibrations of

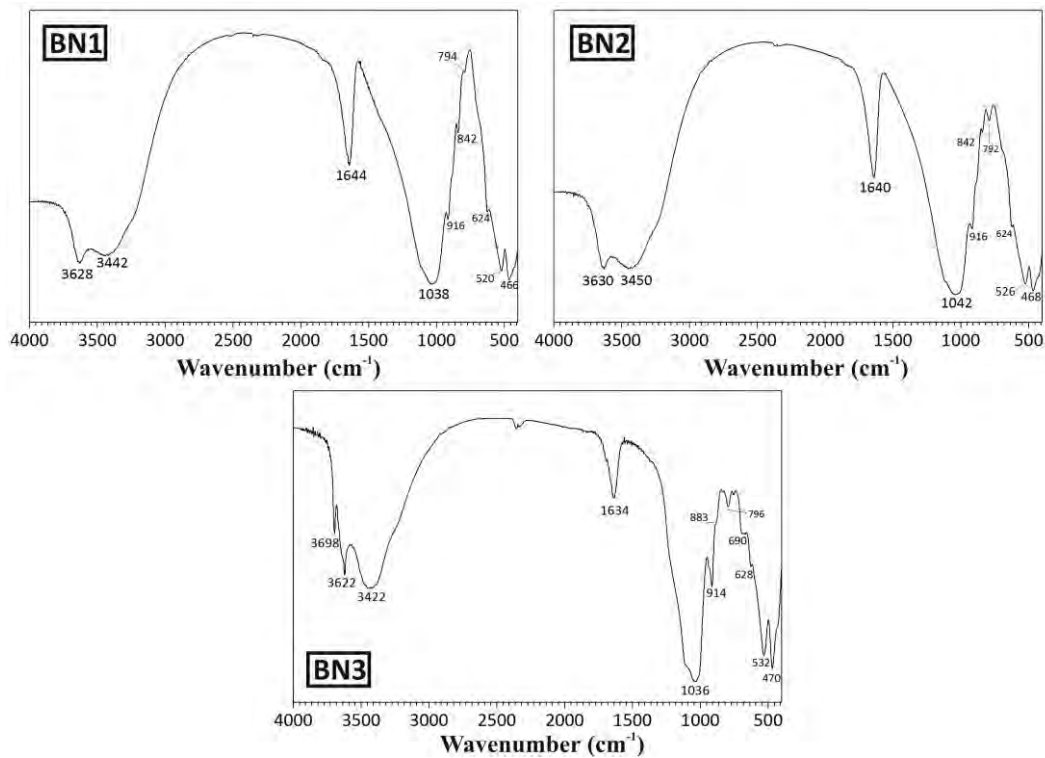


Figure 3 – FTIR spectra of the bentonite samples.

Table 2 – FTIR spectral data of the bentonite samples.

Assignment	Data from previous studies					Bentonite Samples (cm <sup>-1</sup> )		
	1 <sup>a</sup>	2 <sup>b</sup>	3 <sup>c</sup>	4 <sup>c</sup>	5 <sup>d</sup>	BN1	BN2	BN3
u (X-O-H) of kaolinite impurity	-	-	-	-	-	-	-	3698
u (X-O-H), X=Al, Mg	3631	3630	3630	3631	3620	3628	3630	3622
u (H-O-H)	3432	3450	3425	3421	3400	3442	3450	3422
δ (H-O-H)	1640	1640	1635	1632	1640	1644	1640	1634
CaCO <sub>3</sub> impurity	-	-	-	1426	-	-	-	-
u (Si-O)	1090	1087	1118	1108	-	-	-	-
u (Si-O-Si)	1045	1041	1043	1054	-	1038	1042	1036
δ (Al-Al-OH)	919	916	920	919	918	916	916	914
δ (Al-Fe-OH)	-	-	883	878	875	-	-	883
δ (Al-Mg-OH)	843	843	848	-	845	842	842	-
u (Si-O) of SiO <sub>2</sub> impurity	798	795	796	796	-	794	792	796
Al-O, Si-O out of plane vibrations	-	624	-	623	-	624	624	628
δ (Si-O-Al <sup>VI</sup> )	524	521	528	525	516	520	526	532
δ (Si-O-Si)	465	471	467	468	467	466	468	470

u: stretch vibration, δ: bending vibration

1: Wyoming bentonite, 2: Ünye bentonite (Turkey), 3,5: Ankeria bentonite (Milos, Greece), 4: Aspro Horio bentonite (Milos, Greece)

<sup>a</sup> Tabak et al., 2007, <sup>b</sup> Sakizci et al., 2010, <sup>c</sup> Christidis et al., 1995, <sup>d</sup> Perraki and Orphanoudaki, 1997

structural OH groups of bentonites (Madejova, 2003; Eren and Afsin, 2008; Caglar et al., 2009; Alabarse et al., 2011; Holtzer et al., 2011). The band at  $3698\text{cm}^{-1}$  observed in sample BN3 is characteristic for kaolinite which is present as impurity in the sample and is frequently used for identification of kaolinites in raw materials. This band is well separated from absorption bands of most other minerals, which allows identification of very low amounts of kaolinites (Joussein et al., 2001; Madejová et al., 2002). The broad band near  $3420\text{cm}^{-1}$ , observed in the spectra of all samples is due to O-H stretching vibrations of adsorbed water, while the bending vibration of water observed at  $1644$ ,  $1640$  and  $1634\text{cm}^{-1}$ , respectively (Xu et al., 2000; Madejova, 2003).

The IR spectra of dioctahedral smectites show only one broad band in the  $1040\text{-}1020\text{cm}^{-1}$  region due to Si-O stretching vibrations. The bands at  $916$  and  $914\text{cm}^{-1}$  are attributed to Al-Al-OH bending vibration, while the band at  $842\text{cm}^{-1}$  observed in the BN1 and BN2 samples corresponds to Al-Mg-OH bending vibration (Madejova, 2003; Eren and Afsin, 2008; Caglar et al., 2009). The peak at  $883\text{cm}^{-1}$  observed in bentonite BN3 could be ascribed to Al-Fe-OH bending vibration (Madejova, 2003). The appearance of two peaks at about  $915\text{cm}^{-1}$  ( $\delta\text{AlAlOH}$ ) and about  $843\text{cm}^{-1}$  ( $\delta\text{AlMgOH}$ ) reflect partial substitution of octahedral Al by Mg in the samples BN1 and BN2. Si-O stretching of quartz ( $\text{SiO}_2$ ) impurity appears at  $794$ ,  $792$  and  $794\text{cm}^{-1}$ , respectively (Caglar et al., 2009; Davarcioğlu and Çiftçi, 2009). The bands at  $520$ ,  $526$  and  $532\text{cm}^{-1}$  are due to the Si-O-Al<sup>VI</sup> bending band (Al<sup>VI</sup> is Al in octahedral positions), while the  $466$ ,  $468$  and  $470\text{cm}^{-1}$  bands to the Si-O-Si bending vibration which is characteristic for smectites (Madejova, 2003). When compared to FTIR data of Miloan bentonites from previous studies (Christidis et al., 1995; Orphanoudaki and Perraki, 1997) and bentonites which have formed in different geological environments like Wyoming and Ünye bentonites, almost identical data were obtained in the present study. Changes in the vibrational frequencies and intensities of Si-O peaks must be ascribed to changes in the silicate structure such as Si-O bond length, Si-O-Si, angle and the angle through which the silica tetrahedra have rotated and the distance between next-nearest oxygens in the basal plane (Sakizci et al., 2010). Weight percentages of chemical compositions and amount of water of the bentonites under study show some differences compared to bentonites from previous studies. Due to these alterations it is not surprising to see some small shifts in the compared data in Table 2.

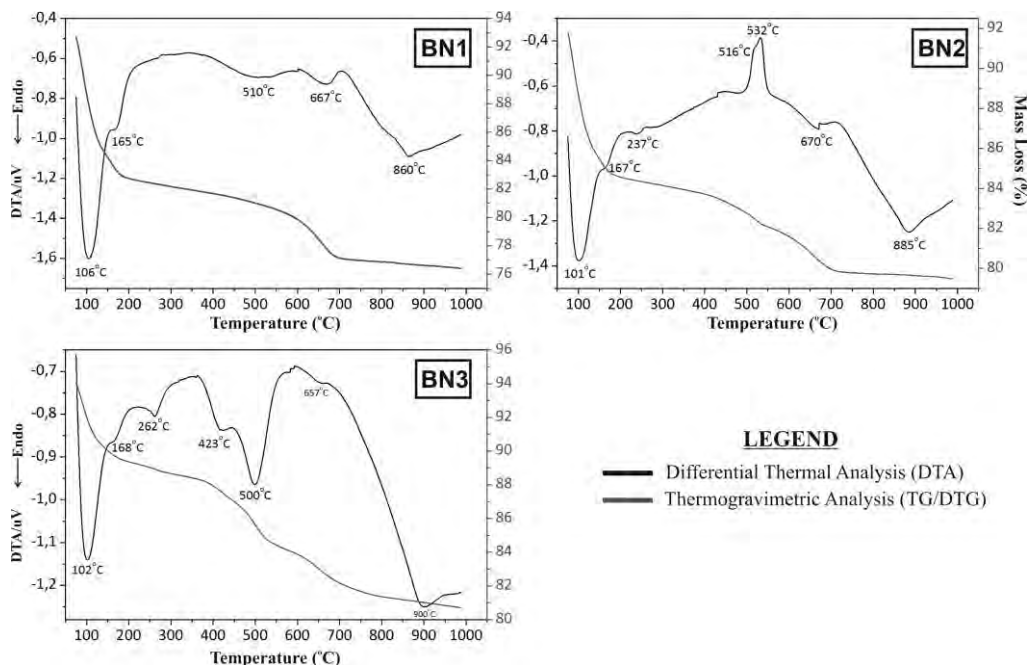


**Figure 4 – Differential thermal analysis (DTA) and thermogravimetric analysis (TG) curves for the bentonite samples.**

### 3.5. Thermal Properties

Physical, physicochemical and/or chemical transformation taking place with the application of a thermal effect, are displayed as endo-/exothermic peaks in relation to temperature. Thus, the respective endo- or exothermic peaks shown in DTA curves are very useful ways to establish transformations with or without mass loss and have been used as one of the major tools for qualitative clay characterization (Sakizci et al., 2009). DTA/TG curves of the bentonites are given in Figure 4 for temperature range of 75–1000°C and the related mass losses are given in Table 3.

The DTA curves, shown in Figure 4, exhibit a low-temperature strong endothermic peak at 106°C for the B1 sample, corresponding to the desorption of physically adsorbed water (Greene-Kelly, 1957; Köster, 1993). There is another very weak endothermic peak, around 165°C, related to the water molecules bound to Ca<sup>2+</sup> cations (Sakizci et al., 2009; Bayram et al., 2010). The endothermic peaks at 510 and 667°C represent the dehydroxylation of structural OH groups (Caglar et al., 2009). The weak endothermic peak at 860°C could be ascribed to structure decomposition. Christidis and Markopoulos (1995) reported complete destruction of the smectite structure between 900°C and 940°C. The DTA–TG curve related to the B1 exhibited a total of four mass losses up to 1000°C is 16.25% for the B1 sample.

**Table 3 – Thermal analysis (DTA/TG) data of the bentonite samples.**

Sample	Temperature Range (°C)	Peak Temperature (°C)	Mass Loss (%)
BN1	75-140	106	8.02
	140-225	165	2.11
	350-540	510	1.26
	540-725	667	3.64
BN2	75-130	101	5.59
	130-225	167	1.80
	350-540	516, 532 (exo)	1.78
	540-725	670	2.34
BN3	75-125	102	3.38
	125-325	168, 262	2.14
	340-450	423	1.55
	450-540	500	2.45
	540-750	657	2.87

B2 bentonite sample exhibits four mass loss events on heating in simultaneous DTA/TG (Figure 4 and Table 3). Two dehydration stages with a total mass loss of 7.39% over the temperature range of 75–225°C are noticeable on the TG curve of B2 sample. The removal of adsorbed water with a mass loss of 5.59% in the first stage 75–130°C gives rise to an endothermic DTA peak centered at 101°C and the endothermic peak at 167°C in the range of 130–225°C which is accompanied by a mass loss of 1.80% corresponds to the elimination of the water species coordinated to the interlayer cations. The endothermic peak at 670°C represents the dehydroxylation of structural OH groups. The endothermic peak at 670°C is associated with 2.34% mass loss in the range of 540–725°C. According to Christidis and Markopoulos (1995) the temperature of the major dehydroxylation for bentonite sample from Aspro Horio quarry was found to be between 685°C



and 690°C. The two superimposing exothermal reactions at 516 and 532°C could be ascribed to the presence of pyrite in this sample (Bonamartini Corradi et al., 1996).

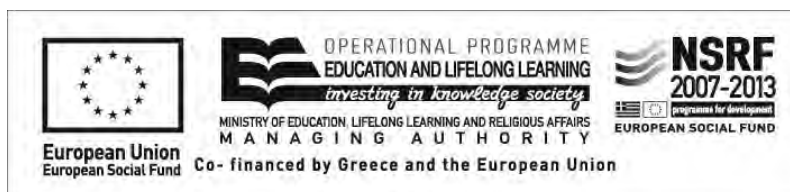
The evolution of adsorbed and cation-coordinated water species in B3 bentonite (Figure 4 and Table 3) is represented by three endothermic peaks at 102, 180 and 262°C, in the range of 75–325°C with a 5.52% mass loss (Figure 4 and Table 3). In DTA plot, a characteristic doublet of endotherms of dioctahedral smectite that appears at 423 and 657°C and are accompanied by a total mass loss of 6.87% in the range of 340–750°C denotes dehydroxylation of B3 bentonite. The strong endothermic reaction at 500°C is attributed to the dehydroxylation of kaolinite detected in this sample (Smykatz-Kloss, 1974).

#### 4. Conclusions

In the present work, characterization of bentonite samples was performed using XRD, AAS, DTA, TG, FT-IR and surface area measurement methods. The XRD results of this investigation show that the clay deposits from Milos island, mainly consist of smectite and specifically Ca-montmorillonite with minor amounts of other clay minerals such as illite and kaolinite and quartz and calcite as impurities. The infrared spectrum of these samples confirmed the presence of dioctahedral smectite as the major mineral and quartz as the main impurity. Additionally, kaolinite was detected in the BN3 bentonite sample. The DTA/TG curves of the bentonite samples exhibit intensive endothermic dehydration peaks with one or two shoulders on the side of the peak that faces higher temperatures which characterize smectites with divalent interlayer cations. This comes in agreement with the chemical and mineralogical analysis which proved that the studied bentonites are mainly consisted of Ca-montmorillonites. The dehydroxylation peak doublet between 500 and 700 °C observed in BN1 and BN3 bentonites characterizes smectites with a mixture of both cis- and trans-vacancies in the octahedral sites in contrast to BN2 bentonite which is a smectite with mainly cis-vacant octahedral sheets. The total mass losses up to 1000°C for BN1, BN2 and BN3 were determined as 16.25%, 12.32%, and 13.35%, respectively.

#### 5. Acknowledgments

The authors would like to express their appreciation to the European Social Fund of the European Union and to the Ministry of Education, Lifelong Learning and Religious Affairs of Greece for financing this research in the framework of HERACLITUS II. Additionally, we would like to thank the S&B Industrial Minerals S.A. company for providing the bentonite samples. Finally, two anonymous referees are fully acknowledged for their valuable comments to the manuscript and their constructive suggestions.



#### 6. References

- Alabarse F.G., Conceição R.V., Balzaretto N.M., Schemato F. and Xavier A.M. 2011. In-situ FTIR analyses of bentonite under high pressure, *Applied Clay Science*, 51, 202-208.
- Bayram H., Önal M., Yilmaz H. and Sarikaya Y. 2010. Thermal analysis of a white calcium bentonite, *Journal of Thermal Analysis and Calorimetry*, 101(3), 873-879.
- Bonamartini Corradi A., Leonelli C., Manfredini T., Pennisi L. and Romagnoli M. 1996. Quantitative determination of pyrite in ceramic clay raw materials by DTA, *Thermochimica Acta*, 287, 101-109.

- Caglar B., Afsin B., Tabak A. and Eren E. 2009. Characterization of the cation-exchanged bentonites by XRPD, ATR, DTA/TG analyses and BET measurement, *Chemical Engineering Journal*, 149, 242-248.
- Christidis, G.E. and Markopoulos T. (1995). Mechanisms of formation of kaolinite and halloysite in the bentonite deposits of Milos island, Greece, *Chemie Der Erde*, 55, 315-329.
- Christidis G.E., Scott P.W. and Marcopoulos T. 1995. Origin of the bentonite deposits of eastern Milos, Aegean, Greece: geological, mineralogical and geochemical evidence, *Clays and Clay Minerals*, 43, 63-77.
- Christidis G.E. and Scott P.W. (1996). Physical and chemical properties of bentonite deposits of Milos island, Greece, *Transactions Of The Institute Of Mining And Metallurgy, Section B, Applied Earth Science*, 105, B165-B174.
- Davarcioğlu B. and Çiftçi E. 2009. Investigation of Central Anatolian clays by FTIR spectroscopy (Arapli-Yesilhisar-Kayseri, Turkey, *International Journal of Natural and Engineering Sciences*, 3, 154-161.
- Eren E. and Afsin B. 2008. An investigation of Cu(II) adsorption by raw and acid-activated bentonite: A combined potentiometric, thermodynamic, XRD, IR, DTA study, *Journal of Hazardous Materials*, 151, 682-691.
- Greene-Kelly R. 1957. The Montmorillonite Minerals (Smectites). In: Mackenzie R. C. (Ed.), *The Differential Thermal Investigation of Clays*. Mineralogical Society, London.
- Grim R.E. 1968. *Clay Mineralogy*, 2<sup>nd</sup> Ed., McGraw Hill, New York.
- Grim R.E. and Góven N. 1978. Bentonites, Geology, Mineralogy, Properties and Uses: *Development in Sedimentology*, Elsevier, Amsterdam.
- Holtzer M., Bobrowski A. and Zymankowska-Kumon S. 2011. Temperature influence on structural changes of foundry bentonites, *Journal of Molecular Structure*, 1004, 102-108.
- Joussein E., Petit S. and Decarreau A. 2001. Une nouvelle méthode de dosage des minéraux argileux en mélange par spectroscopie IR, *Comptes Rendus de l'Académie des Sciences*, 332, 83-89.
- Kogel J.E., Trivedi N.C., Barker J.M. and Krukowski S.T. 2006. Industrial minerals and rocks: commodities, markets, and uses, *Society for Mining, Metallurgy, and Exploration, INC. (SME)*, USA.
- Köster H. M. 1993. Dreischichtminerale oder 2:1 Schichtsilikate. In: Jasmund K. & Lagaly G. (Eds.), *Tonminerale und Tone*. Darmstadt: Steinkopff Verlag.
- Madejova J. 2003. FTIR techniques in clay mineral studies, *Vibrational Spectroscopy*, 31, 1-10.
- Madejová J., Kečkéš J., Pálková H. and Komadel P. 2002. Identification of components in smectite-kaolinite mixtures, *Clay Minerals*, 37, 377-388.
- Murray H.H. 1991. Overview-clay mineral applications, *Applied Clay Science*, 5, 379.
- Murray H.H. 2000. Traditional and new applications for kaolin, smectite and palygorskite: a general overview, *Applied Clay Science*, 17, 207.
- Perraki T. and Orphanoudaki A. (1997). Etude de la composition mineralogique et de proprietes physiques des bentonites de l'île de Milos (Grece), *Mineral Wealth*, 104, 35-42.
- Sakizci M., Alver B.E., Alver O. and Yörükoğullari E. 2010. Spectroscopic and thermal studies of bentonites from Ünye, Turkey, *Journal of Molecular Structure*, 969, 187-191.
- Sakizci M., Alver B.E. and Yörükoğullari E. 2009. Thermal behaviour and immersion heats of selected clays from Turkey, *Journal of Thermal Analysis and Calorimetry*, 98, 429-436.
- Smykatz-Kloss W. 1974. *Differential Thermal Analysis*, Springer-Verlag, Berlin, 185 pp.
- Tabak A., Afsin B., Caglar B. and Koksal E. 2007. Characterization and pillaring of a Turkish bentonite (Resadiye), *Journal of Colloid and Interface Science*, 313, 5-11.
- Volzone C. and Ortiga J. 2000. O<sub>2</sub>, CH<sub>4</sub> and CO<sub>2</sub> gas retentions by acid smectites before and after thermal treatment, *Journal of Materials Science*, 35(21), 5291.
- Xu W., Johnston C.T., Parker P. and Agnew S.F. 2000. Infrared study of water sorption on Na-, Li-, Ca-, and Mg-exchanged (SWy-1 and SAz-1) montmorillonite, *Clays and Clay Minerals*, 48, 120-131.